

# Automated Classification of ROSAT Sources Using Heterogeneous Multiwavelength Source Catalogs

T. A. McGlynn<sup>1</sup>, A. A. Suchkov<sup>2</sup>, E. L. Winter<sup>1,6</sup>, R. J. Hanisch<sup>2</sup>, R. L. White<sup>2</sup>, F. Ochsenein<sup>3</sup>, S. Derriere<sup>3</sup>, W. Voges<sup>4</sup>, M. F. Corcoran<sup>1,5</sup>, S. A. Drake<sup>1,5</sup>,

## ABSTRACT

We describe an on-line system for automated classification of X-ray sources, ClassX, and present preliminary results of classification of the three major catalogs of ROSAT sources, RASS BSC, RASS FSC, and WGACAT, into six class categories: stars, white dwarfs, X-ray binaries, galaxies, AGNs, and clusters of galaxies. ClassX is based on a machine learning technology. It represents a system of classifiers, each classifier consisting of a considerable number of oblique decision trees. These trees are built as the classifier is ‘trained’ to recognize various classes of objects using a training sample of sources of known object types. Each source is characterized by a pre-selected set of parameters, or attributes; the same set is then used as the classifier conducts classification of sources of unknown identity. The ClassX pipeline features an automatic search for X-ray source counterparts among heterogeneous data sets in on-line data archives using Virtual Observatory protocols; it retrieves from those archives all the attributes required by the selected classifier and inputs them to the classifier. The user input to ClassX is typically a file with target coordinates, optionally complemented with target IDs. The output contains the class name, attributes, and class probabilities for all classified targets. We discuss ways to characterize and assess the classifier quality and performance and present the respective validation procedures. Based on both internal and external validation, we conclude that the ClassX classifiers yield reasonable and reliable classifications for ROSAT sources

---

<sup>1</sup>NASA Goddard Space Flight Center, Greenbelt, MD 20771

<sup>2</sup>Space Telescope Science Institute, operated by AURA Inc., under contract with NASA, 3700 San Martin Dr., Baltimore, MD 21218

<sup>3</sup>CDS, Observatoire Astronomique, UMR 7550, 11 rue de l’Université, F-67000 Strasbourg, France

<sup>4</sup>Max-Planck-Institute für Extraterrestrische Physik, 85740 Garching, Germany

<sup>5</sup>Universities Space Research Association, Seabrook, MD 20706

<sup>6</sup>Science Systems and Applications Inc, Lanham, MD 20706

and have the potential to broaden class representation significantly for rare object types.

*Subject headings:* methods: statistical — surveys — X-rays: general — X-rays: binaries — X-rays: stars

## 1. Introduction

The classification of astronomical sources into physically distinct classes is a key element of research in all domains of astrophysics. Traditionally this has involved painstaking manual analysis of detailed, homogeneous sets of observations. More recently automated classifier tools have been used to help in the classification of objects from huge but still largely homogeneous surveys. Examples include analysis of the First (Odewahn 1995) and Second (Weir et al. 1995) Digital Sky Surveys and the Sloan Digital Sky Survey (SDSS; Adelman et al. 1995). In this paper we discuss how we can go beyond using single large surveys and combine information from multiple heterogeneous databases to classify astronomical sources. Using dynamic cross-correlations of electronically available datasets, our ClassX team has developed a series of classifiers that rapidly sort X-ray sources into classes. These facilities are now available to the community at the ClassX web site<sup>7</sup>.

Our initial work has concentrated on the more than one hundred thousand unclassified sources detected by the ROSAT observatory<sup>8</sup> from 1990 to 1999. These high-energy sources are particularly rich in interesting objects: QSOs and other AGNs, clusters of galaxies, young stars, and multiple systems containing white dwarf, neutron star, or black hole companions. The ROSAT samples have been used in prior investigations (e.g., Rutledge et al. 2000; Zhang & Zhao 2003), but still only about 10% of the sources observed by ROSAT have a reliable classification. In most cases this identification rests upon cross-correlation between the ROSAT object and tables of classified sources. In some cases detailed follow-up observations have been performed on a source by source basis. This is extraordinarily expensive in both telescope time and the time of astronomers analyzing these data. Direct comparison of ROSAT sources with massive optical catalogs (e.g., Rutledge, Brunner and Prince 2000) enables the cross-identification of ROSAT sources, but unless the class of the counterpart is known, this does not determine the type of the source. However, using the flux information from multiple catalogs allows us to try to classify sources with more information than is

---

<sup>7</sup><http://heasarc.gsfc.nasa.gov/classx>

<sup>8</sup><http://wave.xray.mpe.mpg.de/ROSAT>

available from the X-ray observations alone.

With the recent and pending publication of several very large datasets covering much of the sky to considerable depth, we have begun to explore how well objects can be classified using data from these large new surveys. The thousands of known sources are used to train classifiers and these trained classifiers are then used to classify the previously unclassified sources. In Section 2 we discuss the sources of information we have used in our classifiers and how we dynamically extract information from the catalogs as needed using capabilities that prototype generic Virtual Observatory tools<sup>9</sup>. Demonstrating the feasibility of this dynamic approach to extracting information was a major technical goal for this project.

Section 3 describes the actual classification tools and the training process we have used. We have used supervised classification technique: oblique decision trees (Murthy, Kasif, & Salzberg 1994). We discuss the reasons for this choice, and the applicability of our approach to other supervised and unsupervised classification algorithms.

Section 4 discusses how we test our classifiers for accuracy. Internal validation looks at the performance of the classifier with respect to the sources we used to train it, and to the general characteristics of our newly classified sources. Can the classifier recover the classes of the data used to train it?

External verification uses data independent of that used to train the classifier and compares how well the classifier predicted these results. Substantial numbers of our sources (several thousand) have been classified by other surveys, notably the SDSS. Comparing our results with these external data sets is a powerful test of our classifiers especially when the external data set is sufficiently deep. We have taken care to consider various selection effects that may affect these tests.

Section 5 gives results for classification of the major ROSAT samples. We show the classification probabilities for each source in our original samples. Since we are classifying nearly 200,000 sources only stubs are included here but the full tables are available for download from the ClassX web site.

The conclusion summarizes the state of the classifiers and describes how we plan to extend our results to other non-ROSAT datasets and to integrate our classifiers in the growing Virtual Observatory.

---

<sup>9</sup>See <http://www.ivoa.net> or <http://us-vo.org>.

## 2. Data Sources and Data Collection

### 2.1. Datasets

#### 2.1.1. WGACAT

The White-Giommi-Angelini Catalog (WGACAT; White et al. 2000) was created by reprocessing the data from the pointed phase observations of the ROSAT PSPC. The result was a catalog of 88,579 sources with X-ray count rates in three energy bands and a variety of supporting data. About 20% of the sources in this sample have classifications derived from cross-correlations with other catalogs. The cross-correlation catalogs are described by White et al. (2000). The cross-correlations were performed from the less specific, i.e., giving only limited information about the type of the counterparts, to more specific catalogs, and the last match was used for the classification. The X-ray positions and fluxes from WGACAT were supplemented with the source extent information derived from the ROSAT PSPC catalog<sup>10</sup>.

The pointed phase of ROSAT PSPC observations lasted nearly 8 years, and during that time the observations provided coverage of about 15% of the sky, with fewer observations at intermediate galactic latitudes. Many regions were observed more than once and objects in those regions may have multiple entries in the WGACAT. When objects shared a common WGACAT ID, only a single value was included in our sample. The catalog contains a quality flag, and the data with higher quality was retained preferentially. In cases with equal quality flags, the entry nearest the center of the field of view was retained. This resulted in a WGACAT sample of 76,763 sources, 18% of which had existing classifications.

X-ray source extent measurements were not included in the WGACAT. We obtained the required data by correlating the WGACAT sources against the ROSAT PSPC (ROSPSPC) catalog, using a correlation radius of 30 arcsec, and selecting the closest candidate as the desired counterpart. In this fashion, X-ray extent information was obtained for 34,633 of the 76,763 distinct WGACAT sources; for the sources without such information the extent parameter was set to zero. The ROSPSPC and WGACAT catalogs were derived from the same set of observations (the pointed phase observations of the ROSAT PSPC instrument), and therefore the source locations and uncertainties are likely a better match between these two catalogs than they would be between WGACAT and survey-phase observations.

Setting the size to 0 where the extent is not known biases the classifier against classes where sources have a real extent, notably clusters of galaxies. However such classes are difficult to pick out of classifiers where the extent is completely omitted, so that this approach

---

<sup>10</sup><http://heasarc/W3Browse/rosat/rospspc.html>

is the most effective way to use the information we have. The presence a ROSAT PSPC catalog counterpart is noted in the tables in section 5.

The distribution of the previously classified sources in both the full WGACAT sample and our subset of it is shown in Table 1. While many objects had more specific classifications (e.g., specific spectral types for stars, or Hubble types for galaxies) the set chosen represent distinct physical origins for the X-ray emission. We felt that understanding classification in these broad categories was necessary before attempting more detailed classifications. These classes in Table 1 represent categories where there were sufficient entries to train the classifier. There were some categories—supernova remnants, nebulae, open star cluster—for which there were only a handful of classified sources. These were eliminated from our training set.

Figure 1 gives the photon count rate distribution for the WGACAT sample for the classified and unclassified sources. While brighter sources are more likely to be classified, there are many classified sources down to the faint end of the observed brightness distribution. The classified sources sample the entire flux space of the WGACAT. Figures 2 and 3 give the overall sky coverage of the WGACAT sources for both the entire sample and the classified sources. Although the WGACAT source distribution is highly non-uniform, there is no major difference between the distributions of the (known) classified WGACAT objects and the entire catalog.

### 2.1.2. *ROSAT All Sky Survey*

The ROSAT All-Sky Survey (RASS) catalogs (Voges et al. 1999) contain X-ray sources detected during the survey phase of the ROSAT mission with the PSPC instrument. The entire sky was surveyed with exposures highest towards the ecliptic poles. While the survey covers the entire sky, it is generally less deep than pointed observations. Overall 124,735 objects were detected: 18,811 of these were published in the RASS Bright Source Catalog (BSC) and 105,924 in the Faint Source Catalog (FSC).

Figures 4 and 5 give the photon count rate distribution of the RASS classified and unclassified sources. Since the classified sources were restricted to the BSC, the sampling of faint objects is quite poor. On the other hand the sky distribution of objects is much more uniform, which is seen in Figures 6 and 7. While there is a marked increase towards the ecliptic poles, the enormous contrasts seen in the sky distribution of the WGACAT sources are not present in this sample.

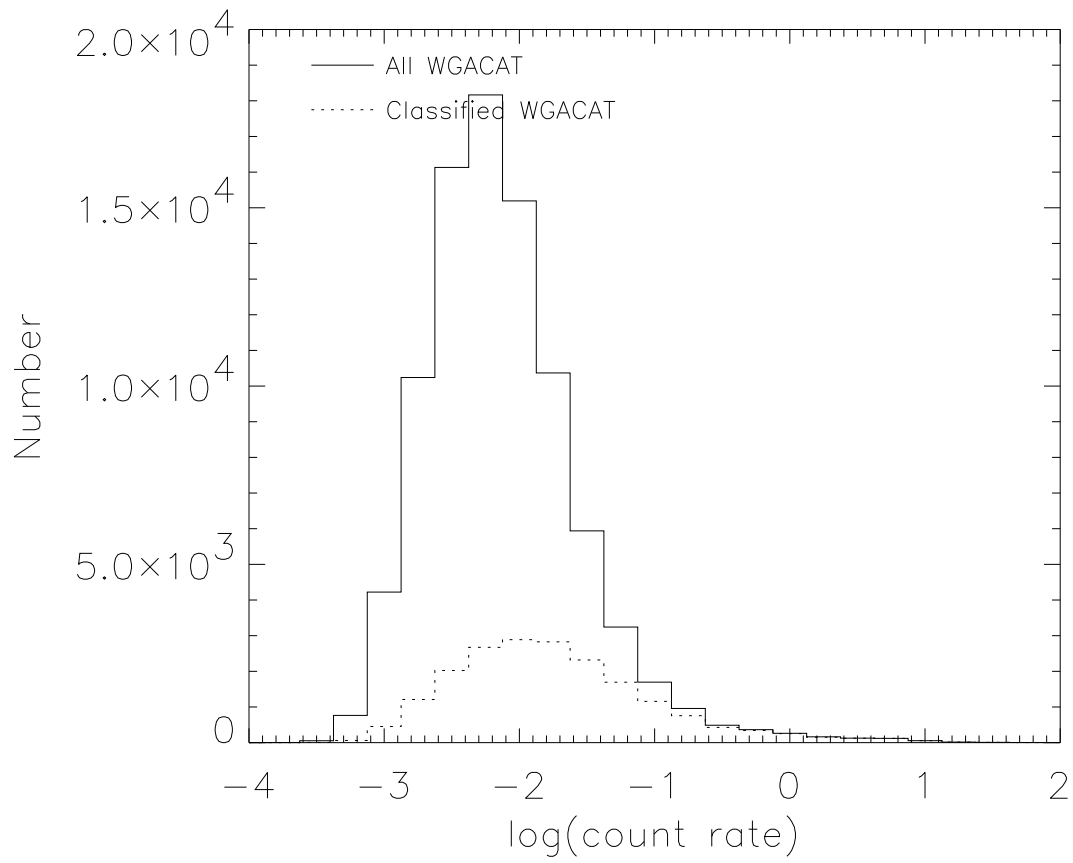


Fig. 1.— Photon count rate distribution for all WGACAT sources (solid line), and classified WGACAT sources (dashed line).

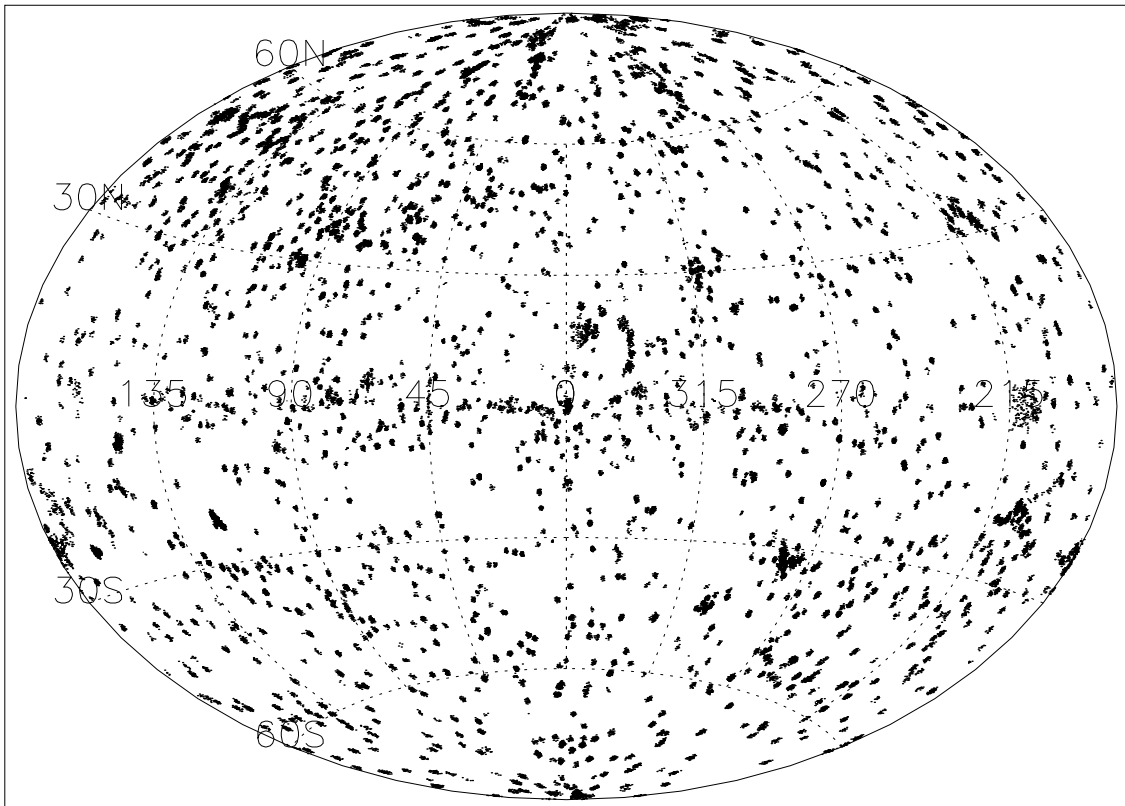


Fig. 2.— Galactic distribution of all WGACAT sources.

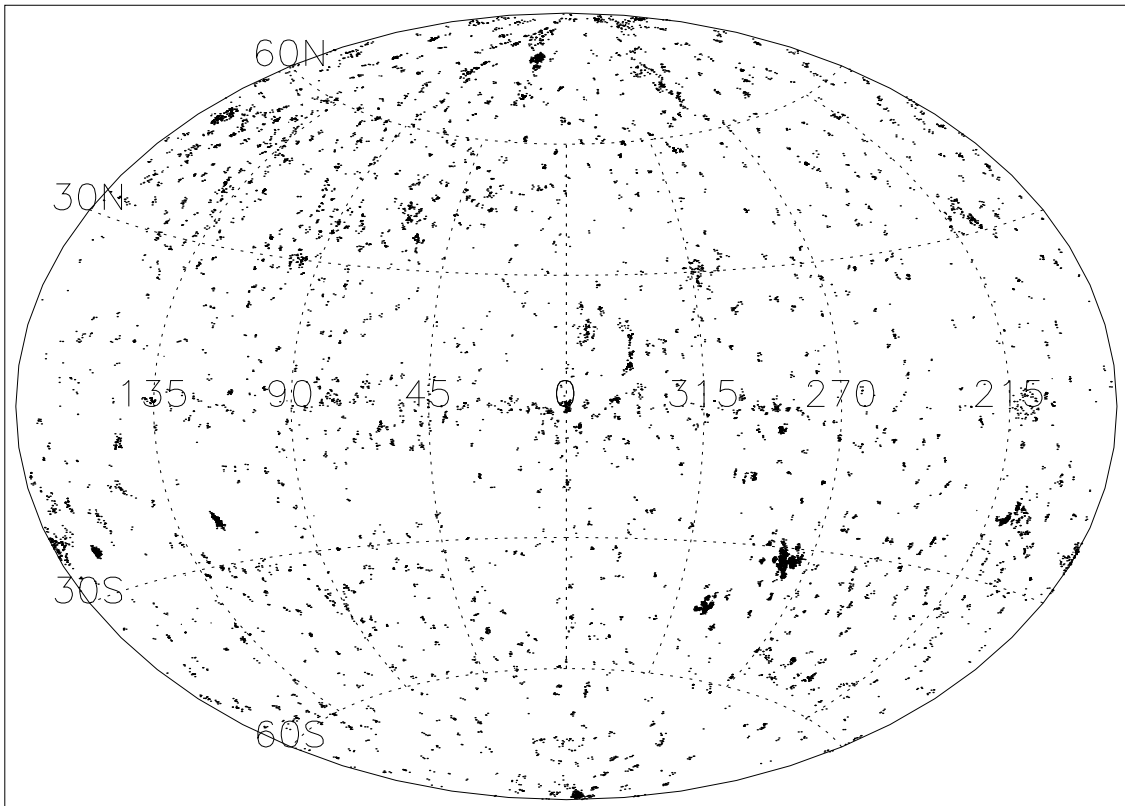


Fig. 3.— Galactic distribution of classified WGACAT sources.



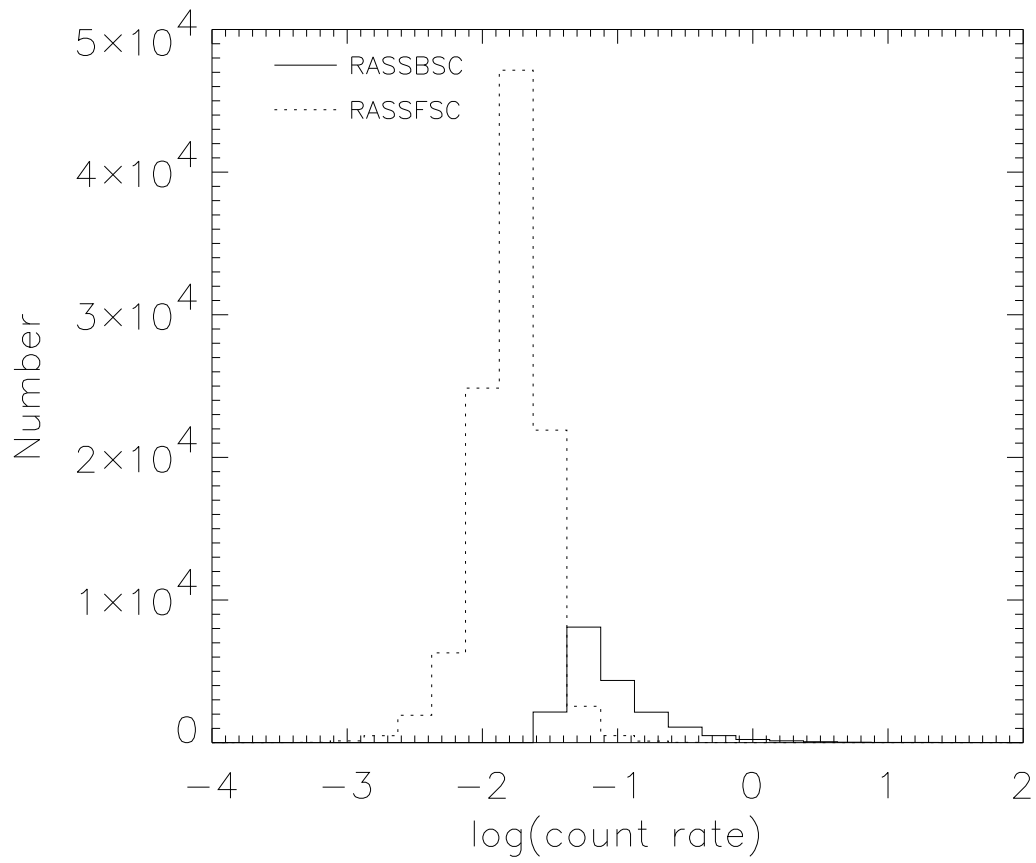


Fig. 4.— Photon count rate distribution for RASS BSC (solid line) and RASS FSC (dashed line) sources.

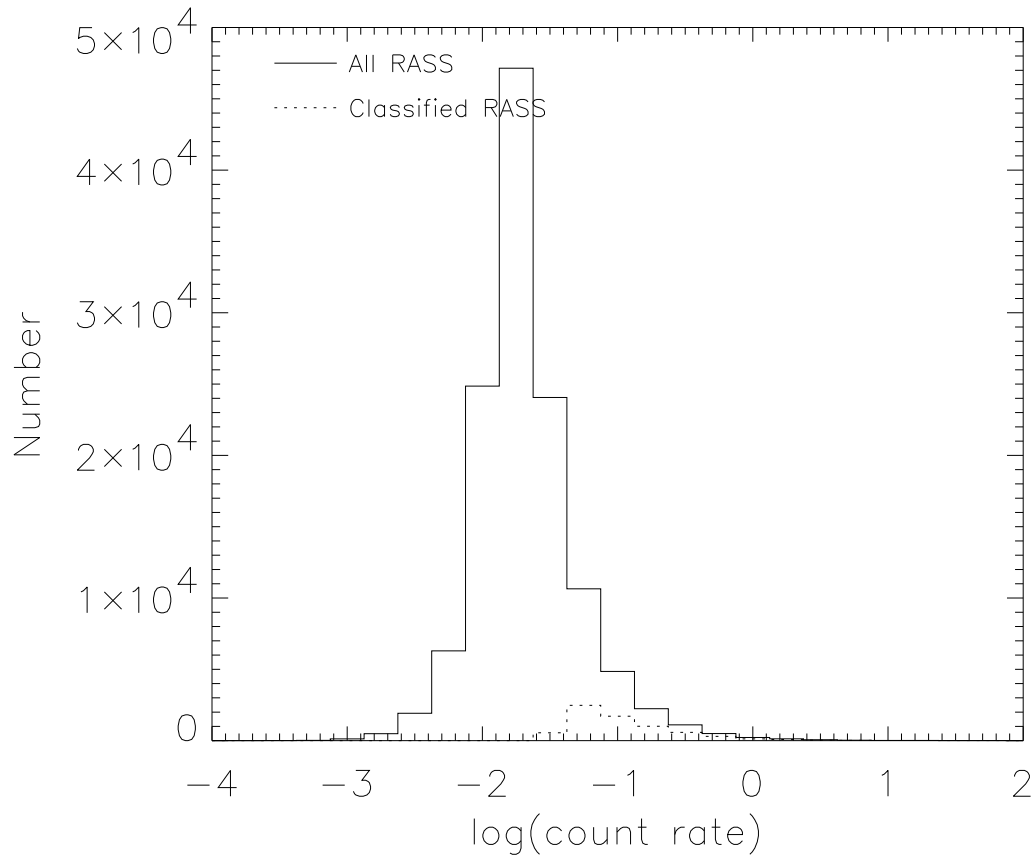


Fig. 5.— Photon count rate distribution for all RASS (solid line) and classified RASS (dashed line) sources.

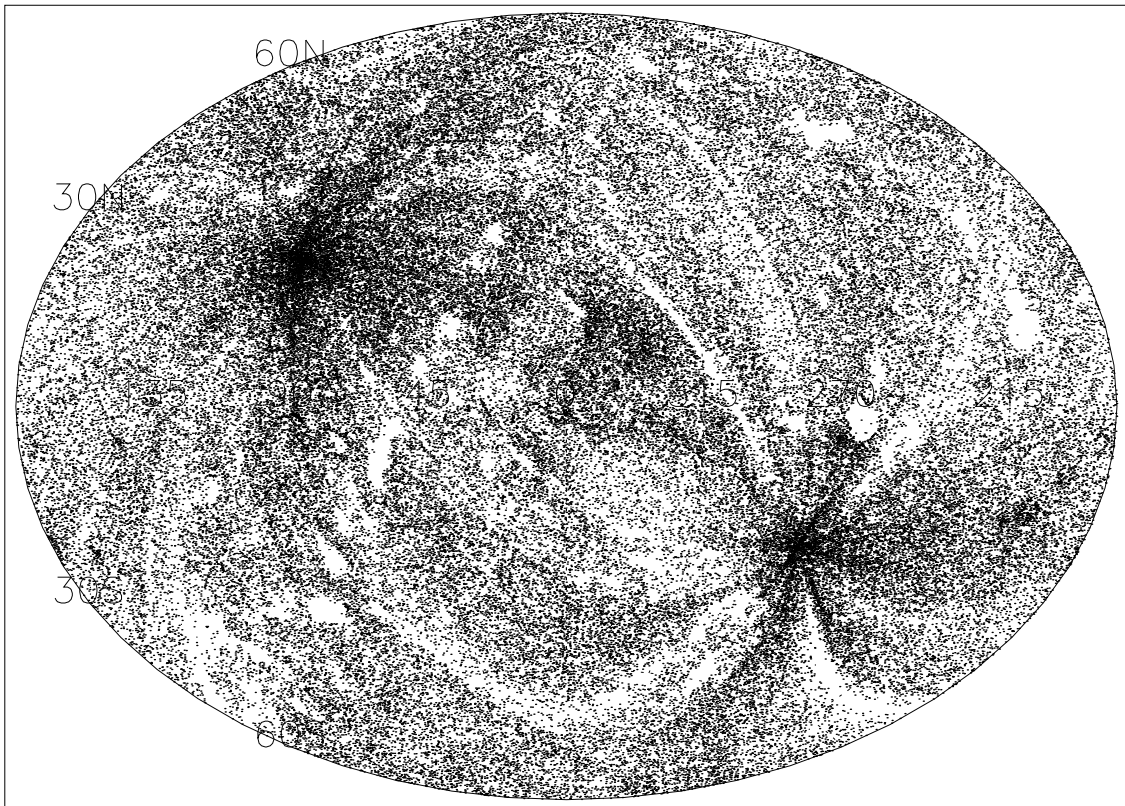


Fig. 6.— Galactic distribution of all RASS sources.

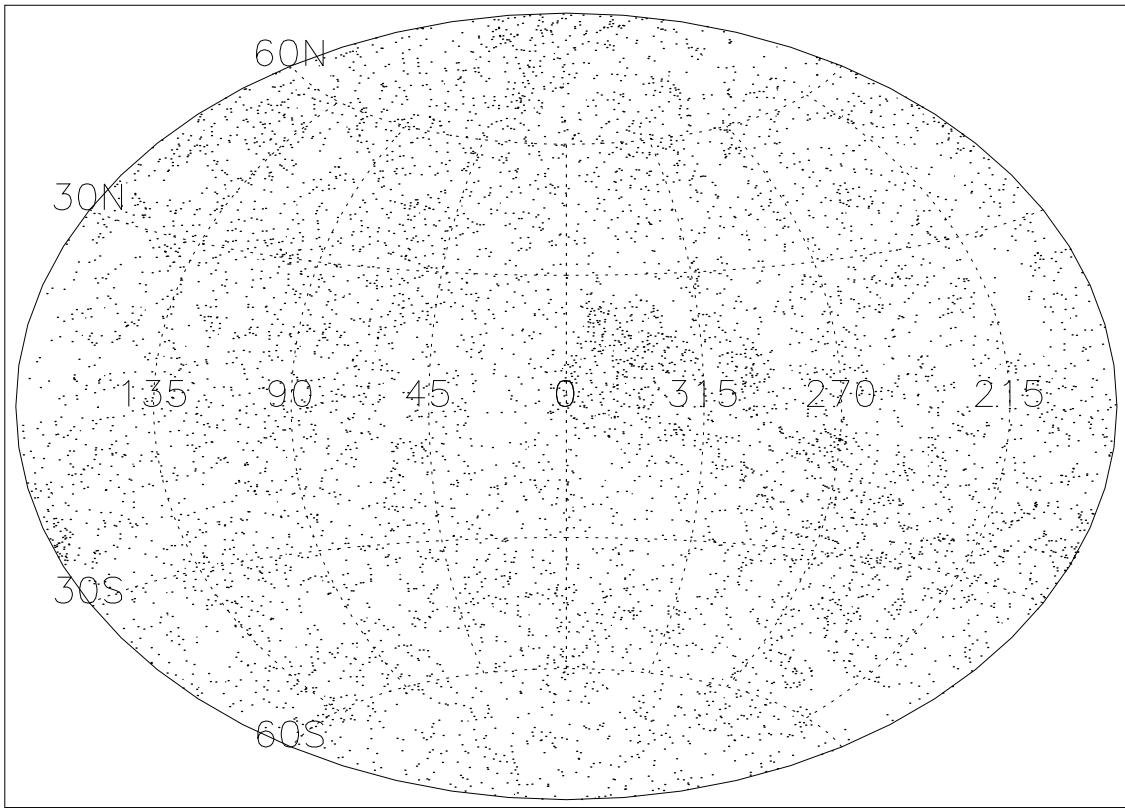


Fig. 7.— Galactic distribution of classified RASS sources.

## 2.2. The ClassX Pipeline

The ClassX processing pipeline gathers the data used for classification. A generic pipeline that can gather data from many catalogs in many wavebands was constructed for ClassX and we have looked at many different sources of information. However in this paper only X-ray, optical, and radio data were used. The catalogs used and information extracted are shown in Table 2. The correlative data from each band is gathered separately, filtered, and then combined to form a single package of data for use by the classifier itself. The classifiers X, and XOR described further in Section 3.5. The ClassX pipeline makes extensive use of the standard representation of tabular and catalog data developed in the Virtual Observatory initiative, VOTable (Ochsenbein et al. 2000).

Optical counterparts of X-ray sources are found using a search radius of 30 arcsec; this gives a reasonable completeness level while keeping the number of chance coincidences manageable. The correlations were done using the VizieR (Ochsenbein, Bauer, & Marcout 2000) system.

If no counterpart was found, the object was dropped from consideration for use by classifiers needing information from that waveband. If a single counterpart was found, then the data from that counterpart was used. When multiple counterparts were found, a rule for resolving the ambiguity was needed. Both nearest and brightest counterparts were tried. Using the brightest counterpart was found to provide generally more accurate results, however, a function combining the two would likely be better still. We have generally used the brightest candidate counterpart.

For radio data, only the existence or non-existence of the radio counterpart was used in the classifier. The combination of the NVSS and SUMSS catalogs gave us radio coverage over approximately 92% of the sky. Since the determination of the coverage boundaries for the SUMSS surveys is non-trivial, data in the 8% region not covered was treated as having no counterpart. Even in classes where radio counterparts are most frequently found, most objects do not have a radio counterpart. So the 8% of the sky remaining does not seem to cause a significant bias.

In the final step before use by the classifier, the data from all tables were combined to produce a pair of files for input to the classifier. Only data for which all parameters required by the classifier were available (either from the table or by use of a default value) were included in the final sample.

### 2.3. Counterpart Validity

The errors in the X-ray positions of the objects in the WGACAT and RASS samples are relatively large compared to the typical separation of objects detected in the USNO-B survey. When we search for optical counterparts to the X-ray sources, we look for the brightest object within 30 arcsec of the nominal X-ray position. Almost all objects have at least one candidate counterpart within 30 arcsec and on average about 5 objects are seen within the limiting radius. How much confidence can we have in the validity of our cross-identification with optical and radio sources? Since we do not perform follow-up observations, this question can only be addressed statistically.

One powerful check on the validity of the identifications is to look for counterparts at positions near but slightly offset from the nominal positions. Both the WGACAT and, to a lesser extent, RASS sources have non-uniform coverage, so that inferences drawn using the statistics of objects over the entire sky are not necessarily appropriate. So in addition to the actual correlation of each object in the WGACAT and RASS samples with the USNO-B survey, we also correlated a point 6 arcmin away at a random position angle. If our cross-correlations were dominated by spurious cross-identifications—i.e., the optical counterparts had no relation to the x-ray sources—then we would expect that the statistics of cross-match between the nominal target positions and the offset positions would be similar. By searching for a set of virtual control objects relatively near the actual objects—much closer than the 2 degree field of view of the ROSAT PSPC—our control sample is subject to the same sample biases as the real data.

It is certainly possible that some X-ray sources may have an extent comparable to our 6 arcmin offset, e.g., clusters of galaxies or nearby galaxies. However this will tend to lessen differences between the nominal and offset samples so that any observed difference between the samples should be considered a lower limit.

Table 3 shows that there are very significant variations between the actual objects and the control sample. The effect is overwhelming in the RASS BSC sample. There the brightnesses of the candidate optical counterparts are about 4 magnitudes greater than for the control sample. A 4 magnitude brightness offset corresponds to a factor of about 200 in the surface density of sources. Clearly the counterparts picked out for the RASS BSC are very special objects so that it seems unlikely that there can be more than a few percent of the counterparts chosen can be unrelated to the X-ray source.

We should note that finding an optical object associated with the X-ray source is distinct from finding the optical counterpart to the X-ray source. For example, consider an X-ray detected cluster of galaxies. Here our procedure might select a particular galaxy in that

cluster as our candidate counterpart. While this galaxy is associated with the X-ray source, it would not be correct to identify the actual source of the observed X-ray emission as a galaxy.<sup>11</sup>

The RASS FSC and WGACAT samples are much deeper so that we would anticipate that counterparts would be fainter. This is borne out in Table 3 but the selected candidate counterparts to the nominal sample are still approximately a magnitude brighter than for the offset control sample. This suggests that while there is some contamination of these samples, most of our candidate counterparts are still associated with the X-ray source. If our optical sources are uniformly distributed in space so that we have a  $b^{-1.5}$  brightness distribution, a one magnitude shift in magnitudes corresponds to a factor of 4 of the surface density of objects. We might expect that 20% of our selected counterparts are not associated with the X-ray source. In many of these cases, the actual X-ray counterpart may have been one of the candidate counterparts but not the brightest within the 30 arcsec radius.

The number of counterparts near the nominal positions is substantially greater than near the offset position. Given that only a tiny fraction of optical objects have X-ray emission detected by ROSAT, we would expect that the number of optical counterparts near the nominal positions would be increased by the number of optical sources associated with the X-ray source, i.e., we get the random background plus the signal. For some X-ray sources there may be multiple optical objects associated with it. For the fainter samples the total number of candidates is roughly consistent with there being one associated optical source for each X-ray object. For the BSC sample, the excess of sources near the nominal positions is substantially greater than the number of objects in the sample so that on average more than 3 optical sources are associated with the X-ray sources. These likely include many clusters of galaxies where a number of galaxies are found near the center of the X-ray emissions.

While we cannot, and do not, assert the validity of any specific positional association, the analysis of the statistical properties of the counterparts assures us that overall, they are dominated by real associations.

---

<sup>11</sup>Since our classifier uses purely empirical techniques, the classifier might still handle such clusters correctly. Even though the cross-identification is ‘wrong’, if this happened consistently the classifier will be trained to correctly recognize these objects as clusters.

### 3. Classification Techniques

#### 3.1. Introduction

*Classification* is the process of mapping the observable characteristics of an object to a set of classes that typically represent different physical types; a classifier is the implementation of a classification algorithm to perform this mapping. We consider here methods for *supervised classification*, meaning that a human expert both has determined into what classes an object may be categorized and also has provided a set of sample objects with known classes. This set of known objects, called the training set, is used by the classification programs to learn how to classify objects. The process of creating such a *classifier* for a particular data set is usually called *training*.

There are also *unsupervised classification* algorithms (e.g., clustering, mixture models) that attempt to determine both the types of objects and how to separate them directly from the parameter-space distribution of the unclassified sample. We have chosen to work primarily with supervised classification methods, however, since we understand much of the underlying physics for the electromagnetic emissions that are measured, and we can thus choose intelligently from among the many measured parameters to build the best training sets and select the best classes.

There are two steps to construct a supervised classifier. In the training phase, the training set is used to decide how the parameters ought to be weighted and combined in order to separate the various classes of objects. In the application phase, the weights determined in the training set are applied to a set of objects that do not have known classes in order to determine what their classes are likely to be.

If a problem has only a few important parameters, then classification is usually an easy problem. For example, with two parameters one can often simply make a scatter-plot of the feature values and can determine graphically how to divide the plane into homogeneous regions where the objects are of the same classes. The classification problem becomes very hard, though, when there are many parameters to consider. Not only is the resulting  $n$ -dimensional space difficult to visualize, but there are so many different combinations of parameters that techniques based on exhaustive searches of the parameter space become computationally infeasible. Practical methods for classification then involve a heuristic approach intended to find a good-enough solution to the optimization problem.



### 3.2. Oblique Decision Trees

There are several ‘dimensions’ that we can vary in building classifiers. The input observational characteristics and the output physical classes can be varied. We can use different sets of training information, and we can vary the basic algorithm for classification. In this paper we report on results using only a single classifier algorithm, the OC1 system of oblique decision trees (Murthy, Kasif, & Salzberg 1994) for a fixed set of output classes. We have chosen the OC1 algorithm because it is freely available<sup>12</sup>, its accuracy is comparable to the best available algorithms, and it is sufficiently fast (in both training and application). An additional benefit is that the decision tree can be examined after it has been trained to determine the key criteria for classification; this is difficult with, for example, neural networks.

Conceptually the oblique decision tree classifier is rather straightforward. It considers the  $n$ -space defined by the set of  $n$  input observational characteristics, where each characteristic is treated as a continuous variable. A binary tree is constructed in which at each node a plane in the  $n$ -space (described by a linear combination of the parameters) divides the objects into two groups. The first node represents a plane that divides the space into two regions. Objects are sifted down the left or right branches of the tree depending on which side of the plane they fall. The next node represents another plane that further divides the two sub-spaces. Ultimately one reaches a leaf node of the tree where all the objects in the region are assigned to a single class. Some parts of parameter space may be well delineated by only a few planes, while other parts might require many planes in order to separate complex distributions.

Oblique decision trees are difficult to construct because there are many possible planes to consider at each tree node. OC1 includes a flexible and efficient algorithm for creating a decision tree given a training set. See the Murthy et al. (1994) paper for full details; we describe here some key features of the algorithm.

OC1 uses a “greedy” algorithm in the initial tree construction. It first attempts to find the plane in the  $n$ -space that most cleanly divides the training set sample into two samples having distinct sets of classes. Various impurity measures are available for determining the quality of a particular split. It then repeats the process recursively for the sub-space on the two sides of the dividing plane. The algorithm continues until each remaining subregion is perfectly classified, with all included training set objects having the same class.

In most cases this initial tree divides the parameter space too finely. For example, some leaf nodes may contain only a single object, picked out by planes that separate it from a

---

<sup>12</sup><http://www.tigr.org/~salzberg/announce-oc1.html>

mass of nearby objects having different classes but with similar parameters. The tree overfits the training set data, tracking details much more closely than is justified. To address this OC1 prunes its decision tree. A fraction of the training set objects is reserved during the initial tree construction. This pruning sample is used to test the decision tree; decision nodes are eliminated if their removal does not reduce the classification accuracy for the pruning sample. The final tree does not classify the training set perfectly (some subregions contain multiple classes of objects), but it has higher overall accuracy than the original overfitted tree.

Oblique decision tree classifiers are not the only possible choices: other commonly used algorithms include neural networks, nearest-neighbor methods, and axis-parallel decision trees. See White (1997, 2000) for discussion of some astronomical applications and a more detailed comparison of these algorithms.

### 3.3. Voting Decision Trees and Classification Probabilities

We have improved on the accuracy of the classification by using not just a single tree, but rather a group of 10 trees that vote (White et al. 2000). This multiple-tree approach has been shown to be effective at improving the accuracy of classifiers (Heath, Kasif, & Salzberg 1996). OC1 uses a complex search algorithm that includes some randomization to avoid the classic problem of getting stuck in local minima in the many-dimensional search space. Thus, one can run OC1 many times using different seeds for the random number generator to produce many different trees.

Heath et al. (1996) used a simple majority voting scheme: classify the object with each tree and then count the number of votes for each class. We have improved on this by using a weighted voting scheme, where each tree splits its vote between classes depending on the populations of the classes from the training set at that leaf. (Recall that after pruning a leaf may contain objects of several different classes.) If an object winds up at a leaf node with  $N$  training set objects of which  $L_i$  are of class  $i$  ( $i = 1 \dots C$ ), the tree’s fractional vote in favor of classification  $i$  is  $(L_i + 1)/(N + C)$ . (The particular form used for the ratio was derived from the binomial statistics at the leaf.) The votes from all 10 trees are averaged to produce a vector of probabilities that an object belongs to each of the possible classes in the training sample. We associate the largest element of this vector with the ‘class’ of the source.

### 3.4. The Output Classes

There are many distinct classes of X-ray sources, and one of the goals of this research is to understand the level of detail to which we can successfully distinguish such sources with the information we have at hand. In practice in this initial effort we have tended to be conservative, using only six basic classes (Table 1).

A problem that needs to be addressed in the classifier design is that the same astronomical object may legitimately belong to very different object types, especially as viewed from different wavelengths. While the X-ray properties of an X-ray binary are likely to be dominated by the accretion onto the compact companion, the optical appearance of the system may be that of, say, a normal B-star—and it may be categorized as such in some catalogs. Similarly, while the X-ray emission of a cluster of galaxies originates mostly in the intracluster gas, the cluster optical or infrared counterpart would typically be a cluster galaxy.

These ambiguities complicate all phases of the classification, including construction of training sets, the training process itself, and interpreting the results. All classification errors are not equally bad when the classes are ambiguous. Clearly if the classifier confuses AGNs with galaxies, this is not nearly as serious as confusing AGNs with stars. We will return to these issues below in our discussion of the results.

### 3.5. ClassX Classifiers

We introduce here four ‘basic’ ClassX classifiers derived from the WGACAT and RASS BSC data (Table 2). They are used in the subsequent discussion to illustrate how the amount and the nature of the information fed into a classifier affects classification results. The RASS-X and WGACAT-X classifiers use ROSAT data only, including positional information. The RASS-XOR and WGACAT-XOR classifiers additionally use optical data for the optical counterparts and a flag indicating whether the source has or does not have a radio counterpart in the NVSS and SUMSS surveys; objects for which no optical counterpart could be found were not used in the training of these classifiers. All four illustrative classifiers are trained to distinguish the same ‘basic’ set of classes: stars, white dwarfs (WD), X-ray binaries (XRB), AGNs, galaxies, and clusters of galaxies.

Many more classifiers are available at the ClassX web site. These include classifiers using correlations with other optical and infrared catalogs, other input parameters, and different sets of output classes.

## 4. Verification

### 4.1. Cross-Validation and Classifier Characterization

The statistical nature of ClassX classifiers means that one has to have some measure of the quality of a classifier to tell if the classification results are of any value. To adequately assess a classifier and interpret classification results one would also need to know what are the differences between the classes and how relevant these differences are in a particular application of the classification results. In the following, we describe some methods to assess the quality of ClassX classifiers, and introduce a quantitative characterization of both the classifiers (e.g., reliability and completeness of classification, classifier preference) and classes (e.g., class affinity).

A natural dataset to use to confirm the quality of a classifier is the training set that was used to develop it. The classifiers are tested using 5-fold cross-validation. The training set is divided into 5 equal-sized, randomly selected subsets (“folds”). Setting aside the first fold, 10 decision trees are constructed by training on the other 4 folds. Then the trees are tested for accuracy on the first fold, which was not used in the training. This process is repeated 5 times, each time holding back a different fold. When this is complete, we have classified the entire training sample. This standard technique avoids the overly optimistic results for classification accuracy one would get if one simply trained the classifier on all the data and then tested it on the same data<sup>13</sup>.

The results of cross-validation can be viewed as a matrix with the input classes as the row headers and the column headers as the output classes (see Table 4). For a perfect classifier, only the diagonal of the matrix would be populated. In practice the ratio of diagonal to off-diagonal elements gives us an immediate sense of how well the classifier has worked. In most cases the accuracy of the classifier is going to be higher for the training set sample than for originally unclassified sources, because the population of unclassified sources may differ systematically from known sources (e.g., by being fainter.) On the other hand, some disagreements between the OC1 classifier and the training set classification are the result of classification errors in the (imperfect) training set. There the cross-validation results correspondingly underestimate the classifier accuracy.

The cross-validation results are shown in Figures 8–9. Each panel in these figures gives the fraction of objects in input class categories classified by ClassX as objects of a given type.

---

<sup>13</sup>Note that classifiers trained with 80% of the data are only used in cross-validation. The classifiers installed at the ClassX web site and used in this paper for classifications of unknown objects are trained using the entire sample of pre-classified sources.

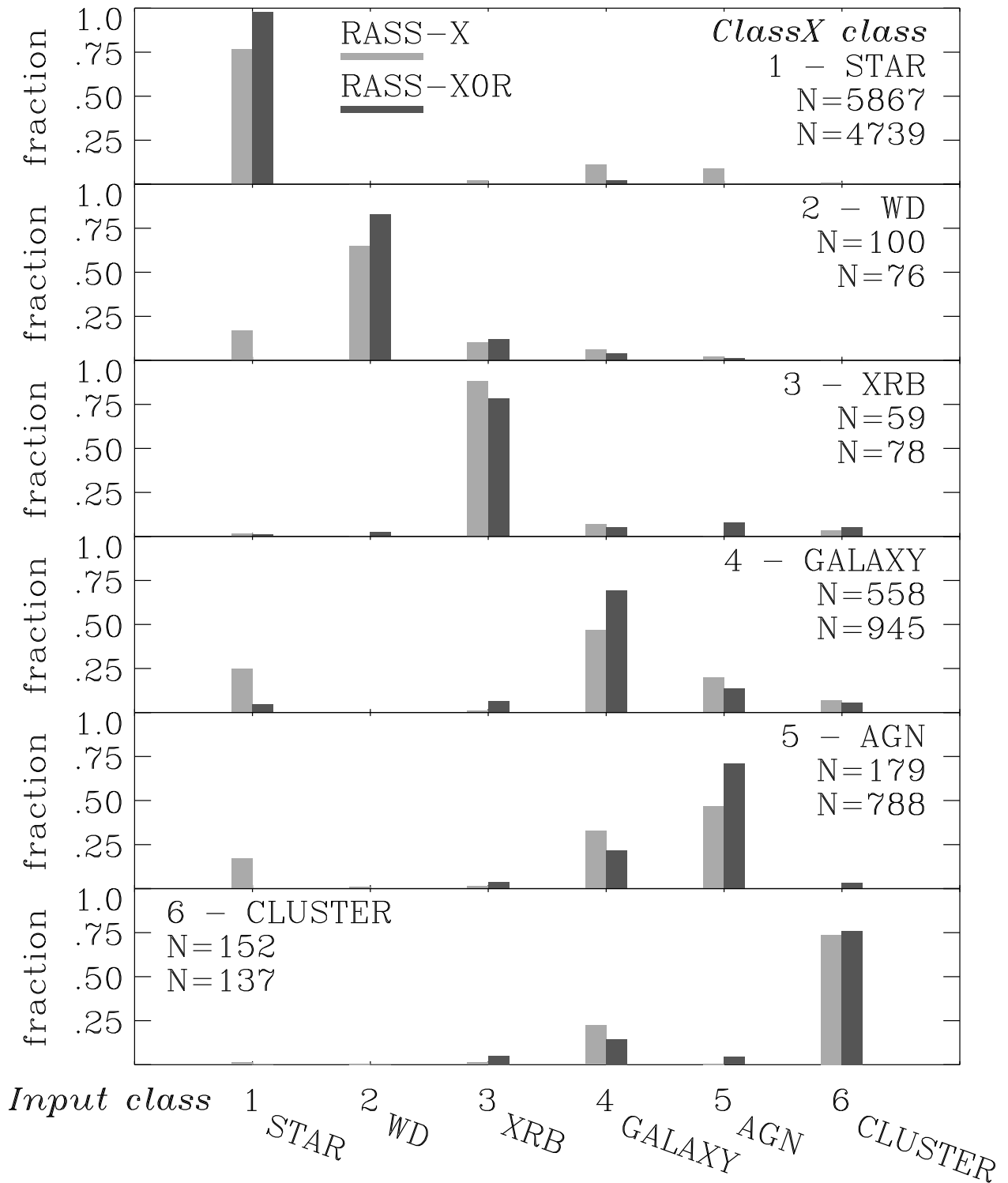


Fig. 8.— Classifier cross-validation: Distribution of input classes within a given ClassX class (class affinity). Light and dark shadings refer to the results for the classifiers using X-ray data only (from ROSAT) and X-ray plus optical and radio data, respectively. Each panel shows the fraction of each of the input classes assigned by ClassX the class name given in the panel. Ideally that fraction must be 100% for the input class having the same name, which means 100% *reliable* classification for that name. In reality, ClassX assigns the given name also to a fraction of objects whose actual class has a different name, which happens

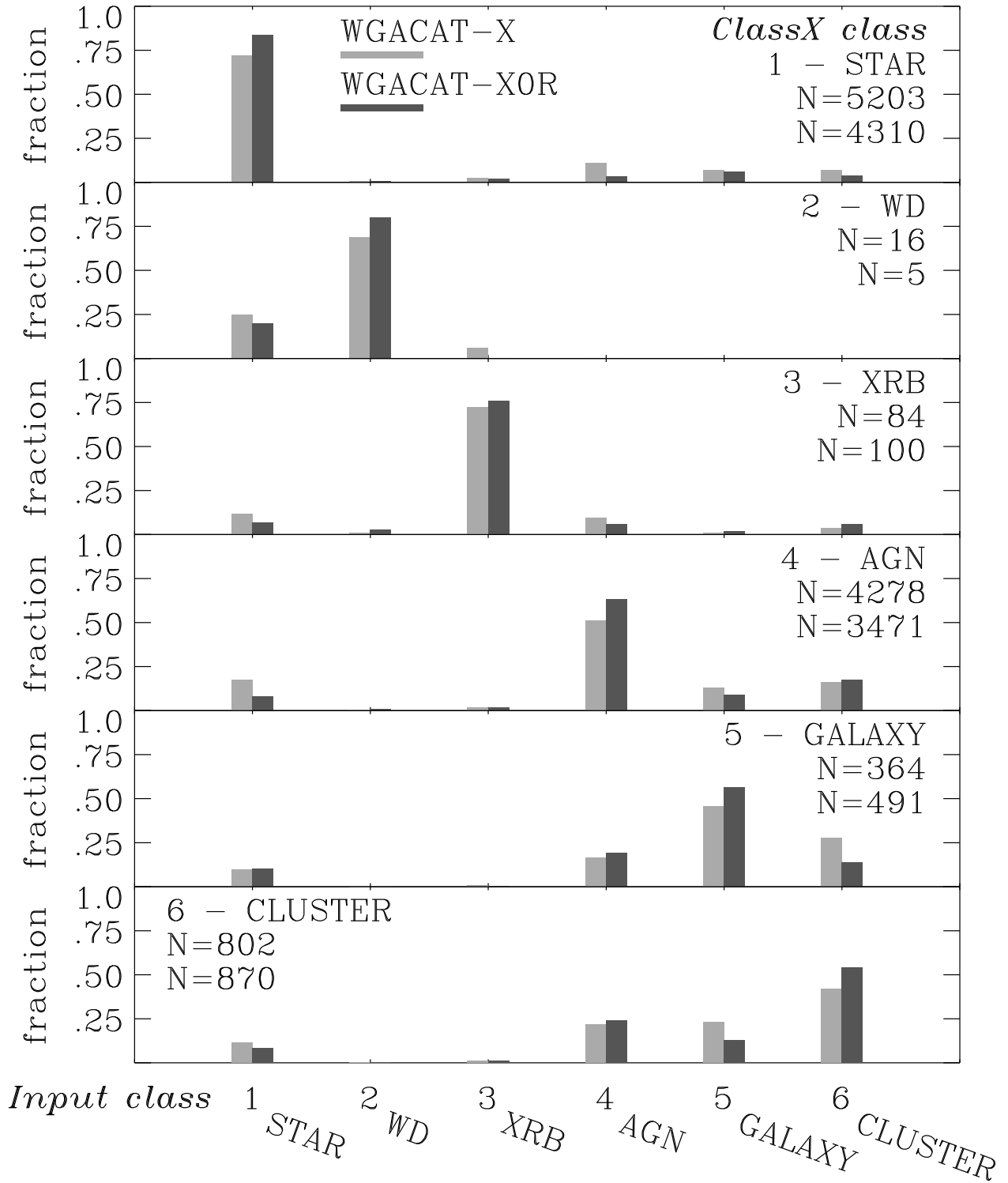


Fig. 9.— Same as in Figure 8 but for the classifiers derived from WGACAT.

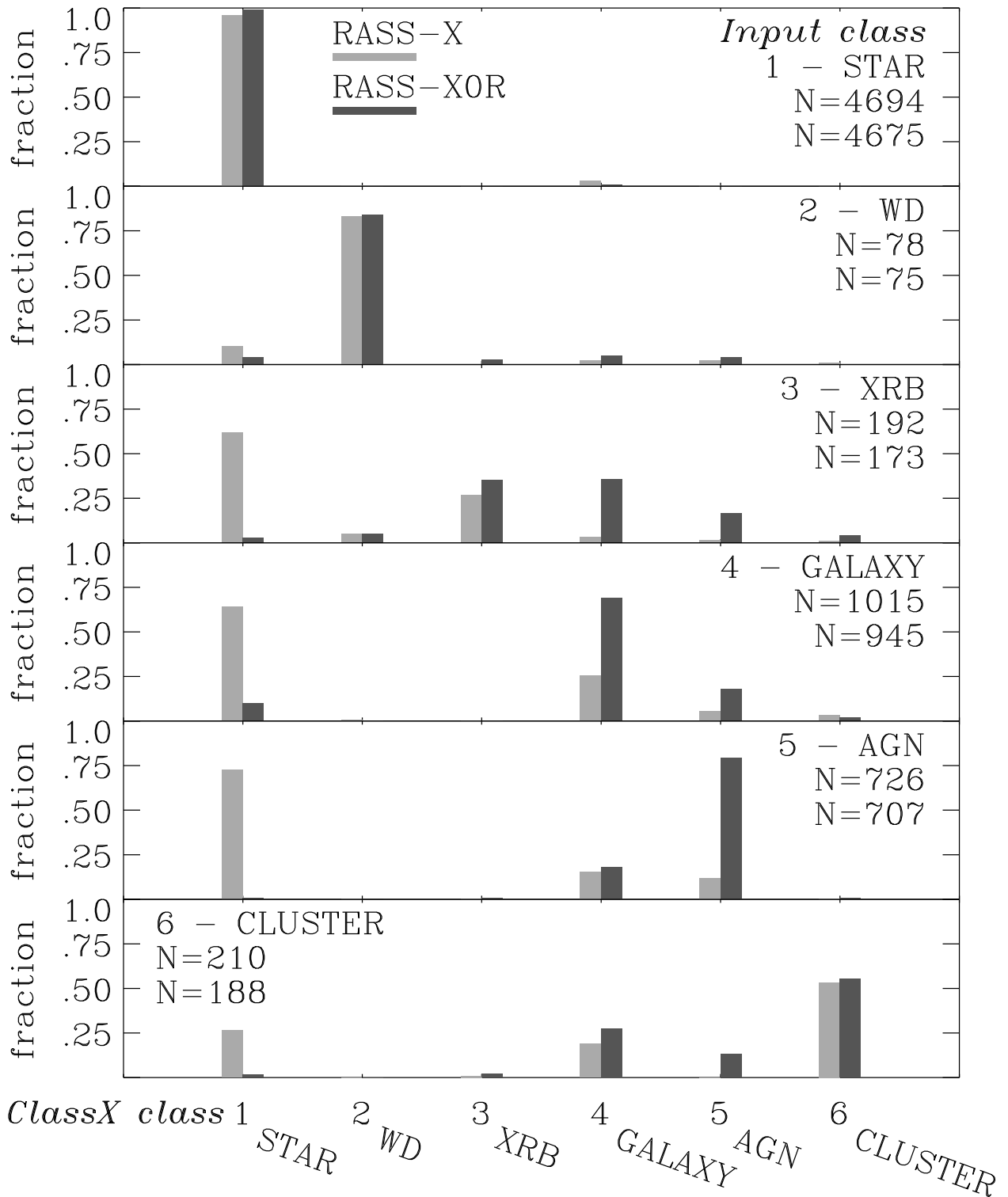


Fig. 10.— Classifier cross-validation: Distribution of ClassX classes within a given input class (classifier preference). Each panel exhibits the fraction of objects of the given input class in each ClassX class. An ideal classifier would assign to all objects in a given input class the name of that class. In reality, the classifier assigns different names, showing different *preference* for different names. In the case of a good classifier, the preference is highest for the name of the given input class.

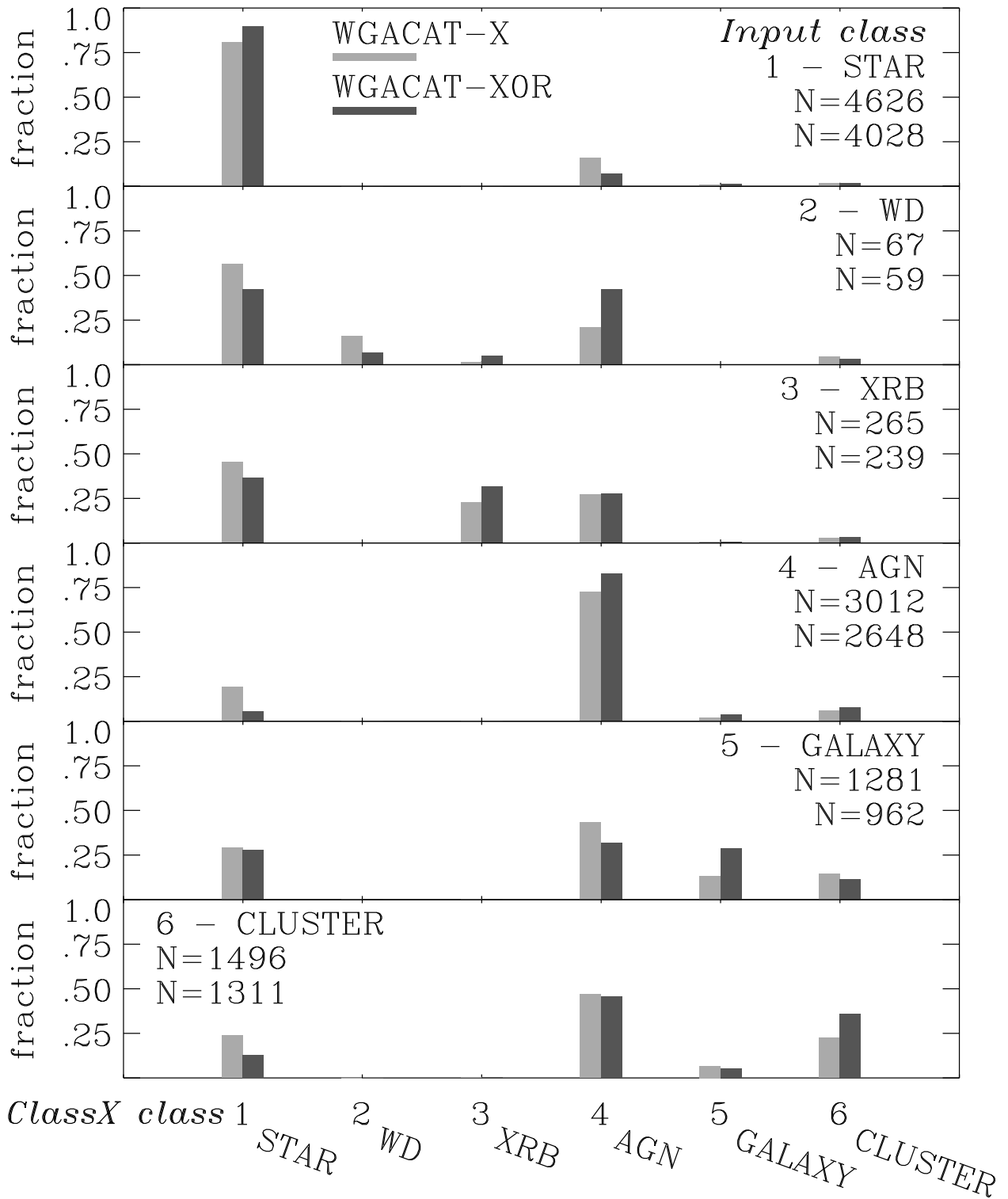


Fig. 11.— Same as in Figure 10 but for the classifiers obtained from the WGACAT training sets.



The diagonal across the panels gives, therefore, the fraction of correctly classified sources in each class and thus represents *reliability* of classification. Because of closeness, or *affinity*, of some classes in the parameter phase space (e.g., galaxies and AGNs), the classifier may place some objects of a given input class into a class with similar properties. Figures 8–9 characterize quantitatively such class affinity. One can infer, for instance, from Figure 8 that there is a substantial affinity between the ROSAT BSC galaxies and AGNs when only X-ray properties are considered. Addition of optical information decreases that affinity quite noticeably. At the same time clusters of galaxies are obviously distinctly different from AGNs in the X-ray. The affinity relationships between the classes are somewhat different for objects from WGACAT (Figure 9).

In Figures 10 and 11, each panel gives the fraction of input objects of a given type classified by ClassX into different class categories. The diagonal across the panels shows us how complete is the placement of sample objects of a given type into the correct class category, giving us a measure of classification *completeness*. In general Figures 10 and 11 show us the classifier *preferences* as it puts objects of a given type into different class categories.

Affinity and preference plots in Figures 8–11 come handy when one want to know what outcome to expect from a particular classification. For instance, from the XRB panel in Figure 10, one would know that less than half XRBs can be expected to get revealed in a sample of X-ray sources. The same panel in the affinity plot, Figures 8, would tell one that 75% or more of sources classified as XRBs are expected to be real XRBs.

The actual counts of objects both in the input and ClassX classes used in cross-validation are given in Table 4. The completeness of the classifier for a particular class is given by the ratio of the diagonal element to the sum of the column. This indicates the fraction of a given class where we recover the correct class. The reliability of the classifier is given by the ratio of the diagonal element to the sum over the row. The normalized row is a measure of affinity of a given class with other classes: for a given input class what class does the automated classification yield? Of course, in both cases we must assume that the original classification is correct.

The cross-validation matrices immediately show many interesting features. When data is misclassified it is usually misclassified into related categories. For instance, clusters or AGNs are misclassified as galaxies and vice versa.

The effect of large samples of one class versus smaller samples of another is also evident. Since there are so many stars, they can significantly pollute samples of galaxies. Even though a classifier may furnish relatively high completeness for a given class, classification reliability for that class would be relatively low when occasional misclassification of a very common

type overwhelms the correct classification of a rare type. The smaller the relative frequency of the object, the more distinctive its observational signature needs to be to stand out against the other classes. For example, white dwarfs are characterized by very soft X-ray spectra. Thus even though they make up only a small subset, they are well handled by our classifiers.

## 4.2. Verification Using External Samples

While the cross-validation results are useful, they cannot address any issues involving the selection of data for the training set itself. We can get some insight into that concern by looking at how well the classifiers handle ROSAT sources of known class that were not in the training set. Using our standard pipelines, we have classified samples of such sources from a number of catalogs containing identified ROSAT objects. Three such samples are discussed below in more detail.

### 4.2.1. *Hipparcos F stars*

Suchkov, Makarov, & Voges (2003) identified 2011 F stars from the *Hipparcos* catalog as X-ray emitters that have X-ray counterparts in the RASS FSC and, to a lesser extent, RASS BSC. Submission of the list of these stars to the classifier RASS-XOR resulted in an output list of 1737 sources, all of which classified as stars (Figure 12). Also a smaller subset of these stars found in the WGACAT by the WGACAT-XOR classifier was all identified as stars. This result is consistent with a very high reliability of star classification for these classifiers as inferred from Figures 8 and Figures 10, thus strongly supporting the credibility of the cross-validation results.

### 4.2.2. *New AGNs from the WGACAT*

P. Padovani (private communication, 2003) supplied us with a sample of 251 WGACAT sources that were identified by him and his collaborators as various types of quasars and AGNs (Landt et al. 2001; Perlman et al. 1998; Padovani et al. in preparation). The results of classification of this sample with the WGACAT-XOR and RASS-XOR classifiers are shown in the middle panel of Figure 12. The classifier does a good job in distinguishing the AGNs from all other classes.

### 4.2.3. *AGNs from the Sloan Digital Sky Survey*

The Sloan Digital Sky Survey (SDSS) is a deep photometric and spectroscopic optical survey, where a large number of sources were spectroscopically identified as AGNs. For more than 1200 Sloan AGNs, Anderson et al. (2003) found X-ray counterparts in the ROSAT All Sky Survey. We used a sample of 964 of these AGNs to test the performance of the ClassX classifiers. The results of the classification of that sample are shown in the lower panel of Figure 12. The classifier performance is very good in terms of differentiating the Sloan AGNs from galactic X-ray sources (stars, white dwarfs, XRBs) and clusters of galaxies. The WGACAT-XOR classifier easily differentiates these AGNs from galaxies; the RASS-XOR classifier is less successful in such a differentiation, possibly because it is trained with substantially brighter objects.

### 4.3. **Classification Accuracy as a Function of Brightness.**

One clear distinction between the classified and unclassified sources is that the classified sources are generally brighter. One may expect that classification accuracy for fainter sources would be different. As one can see in Figure 13, classification accuracy does indeed vary with X-ray brightness. Interestingly enough, the degree and even the sense of that variation is not the same for different classes. In the case of AGNs, the accuracy drops from 80% at the bright end to below 70% at the faint end of the distribution. In contrast the classification accuracy of clusters of galaxies tends to increase rather than decrease toward faint sources. For stars, accuracy variation is rather small, with a slight tendency to accuracy degradation at the faint end. The accuracy variation is obviously important to know for interpretation of classification results, especially when a classifier is used in a parameter domain substantially different from that of the training data.

### 4.4. **Limits and Issues**

While our validation of the classifiers is not entirely secure, especially with regard to the cross-correlation errors and the effects of selection on the training set, several distinct lines of evidence suggest that these classifiers give reasonable classifications for their sources. While no single classifier is optimal for classifying all kinds of data, a classifier network that filters data through a series of classifiers can give reasonable results for a heterogeneous dataset. A scientist with more specialized requirements, such as completeness without regard to purity for galaxies, or perhaps a pure sample of early type stars, may wish to choose a classifier

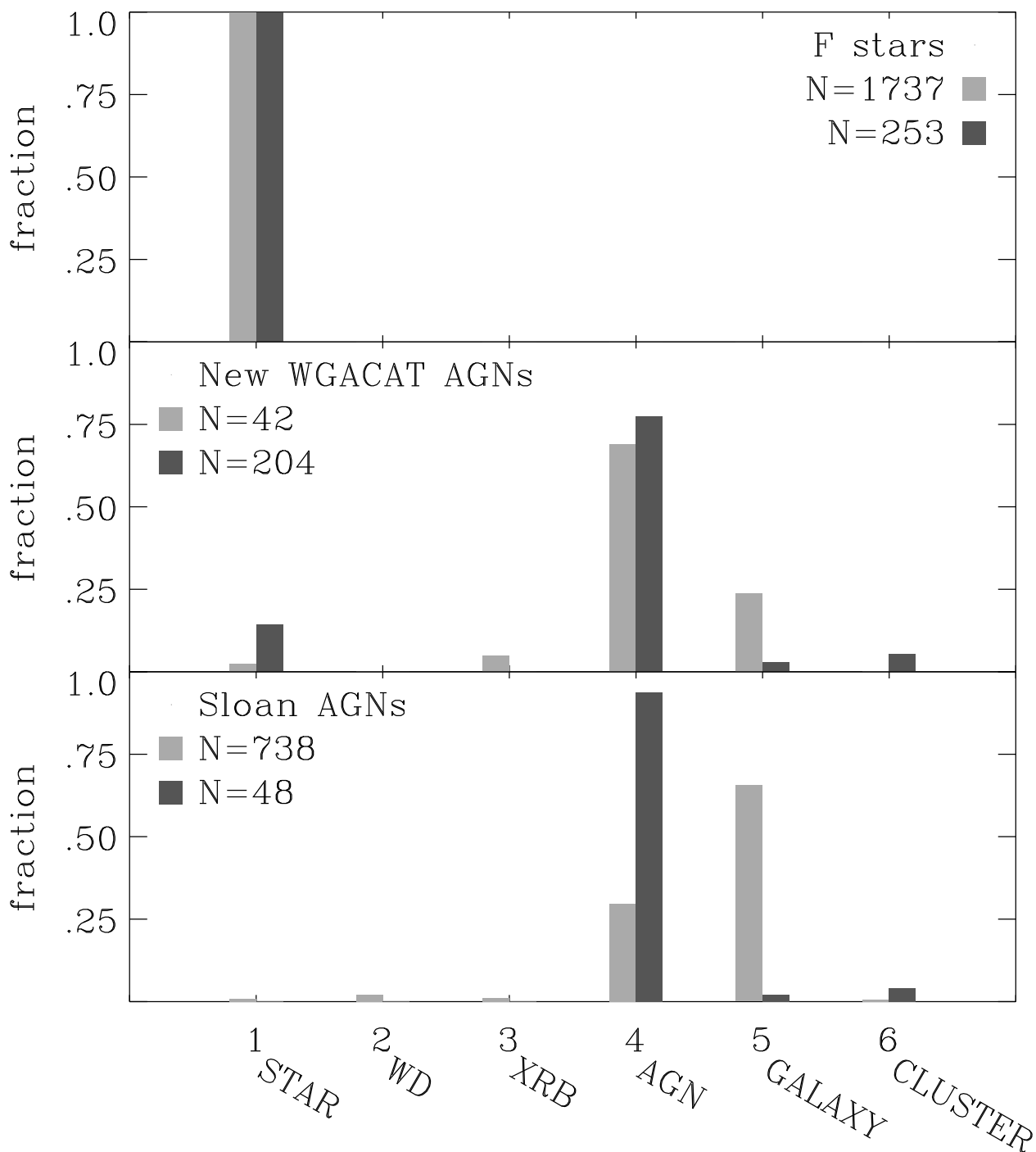


Fig. 12.— Class distribution for a sample of X-ray F stars (upper panel) and two samples of AGNs (middle and lower panels). The samples were classified by the classifiers RASS-XOR (light shading) and WGACAT-XOR (dark shading). Classification shown in light gray in the lower panel is discussed in text. The sample of F stars is from the paper by Suchkov et al. (2003). The sample in the middle panel is due to P. Padovani. It comprises mostly the sources from Landt et al. (2001) and Perlman et al. (1998), which were drawn from the previously unclassified WGACAT sources and identified as AGNs. The sample in the lower panel comprises AGNs from the Sloan Digital Sky Survey that were found to have X-ray counterparts in the ROSAT All Sky Survey catalogs (Anderson et al. 2003).

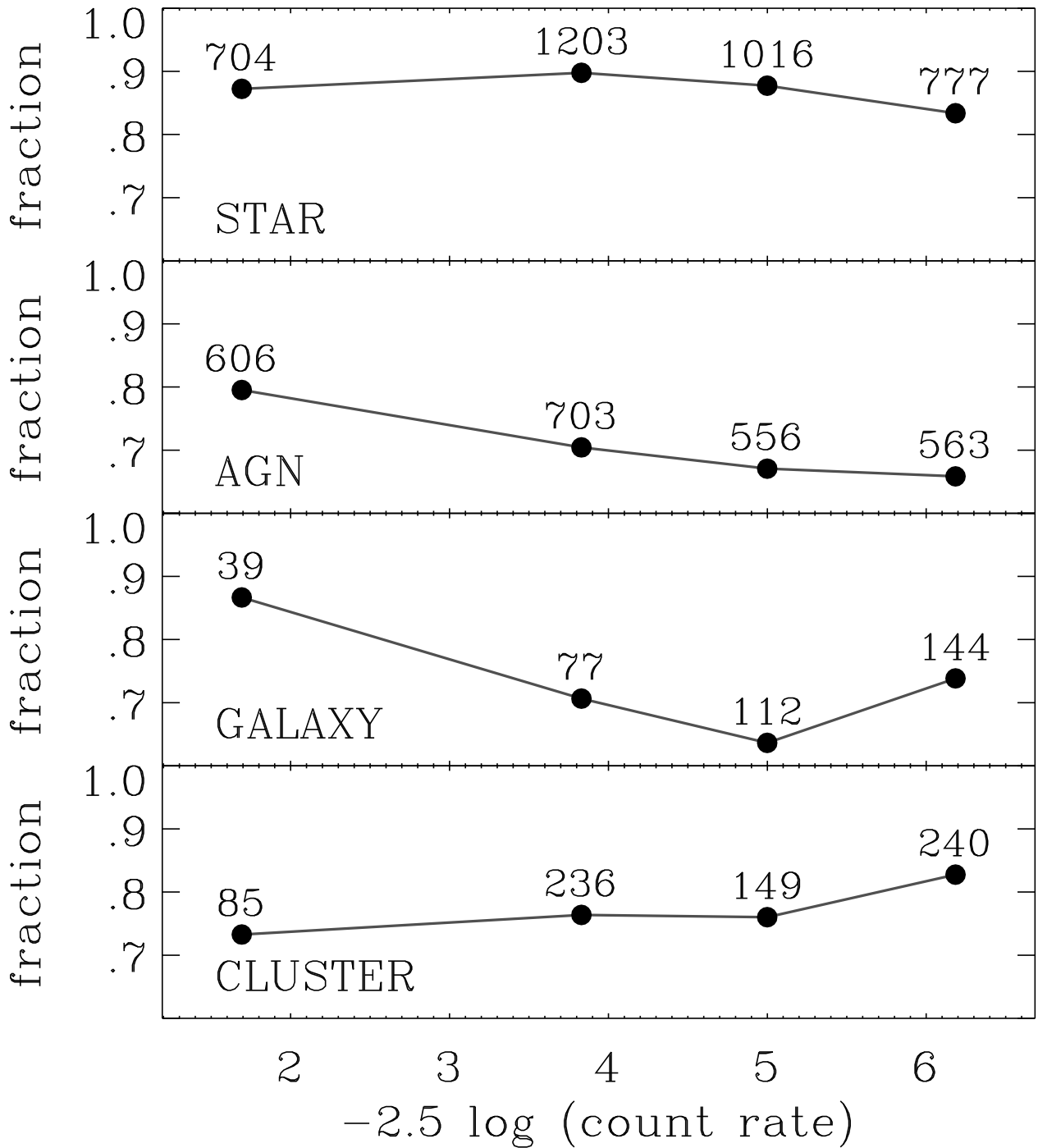


Fig. 13.— Fraction of the WGACAT training set sources correctly classified by the classifier WGACAT-XOR, displayed as a function of X-ray brightness (defined as  $-2.5 \log(\text{count rate})$ ). The actual number of sources of a given class in each brightness bin is also shown.

that optimizes that property.

The classifiers have been built from heterogeneous data sources, which are likely to have some fraction of incorrect identifications. Pruned decision tree classifiers seem to be robust in the face of such contamination, so that one can even use the classifiers to attempt to purify the input data set.

## 5. Summary of Results

Classification results from ClassX for the entire WGACAT and RASS datasets are available at the ClassX web site at <http://heasarc.gsfc.nasa.gov/classx>. They are illustrated in Tables 5 and 6, which show the first few rows of two selected tables.

In addition to these static classifications, more than two dozen ClassX classifiers, readily accessible for the community for immediate use, are currently deployed at the ClassX web site. The web site contains a description of the input data format, which is the list of source coordinates, and the input/output options. All the classifiers are supplied with the information indicating the classifier class categories, parameters (attributes) to be used in classification and returned in the output, databases (catalogs) to be searched for the source information, and other relevant information. In the output, each classified source is supplied with classification probabilities for all classes, and is assigned a class name, which corresponds to the class with the highest classification probability. The output also contains the parameter values retrieved for the source and used in classification.

## 6. Conclusions

Classification of X-ray (or optical, infrared, etc.) sources into various categories of astronomical object types can rarely, if at all, be 100% accurate. The presence of uncertainty inherent to classifications based on statistical methods immediately splits the very goal of classification into a set of different goals, which are often incompatible. As a result, any statement about classifier effectiveness would generally make sense only if the classification goal or task, with respect to which the effectiveness is considered, is indicated. For example, one may want either to isolate as complete as possible objects of a given class in a given sample, even at the expense of a larger fraction of misclassified sources, or to deal only with objects of a class identified with the highest possible degree of reliability, even at the expense of rejecting many class objects that the classifier is unable to identify as such at the desired level of reliability. These different goals can be addressed in ClassX with different classifiers.

One classifier can be effective in identifying to a high degree of completeness the members of a class, but classification reliability for identified class members may not be high enough. Still another classifier can be effective in delivering highly reliable class members but may miss many actual members of the same class.

Supervised classification techniques are a very powerful way of extending information about well-understood objects in a sample to the entire sample. For X-ray sources, it is possible to do classifications using just a few X-ray parameters as object attributes. Multi-wavelength data can substantially improve the quality of the classifications, although adding data without regard to its quality or uniqueness does not necessarily help.

The ClassX classifications are useful for studying classes of objects, but the classification of any individual object should be taken as advisory rather than definitive. Human understanding and judgment is crucial in assessment and interpretations of the results. This is especially true given the statistical nature of ClassX.

In ClassX, a substantial number of input (training) sources are required for each class to effectively classify a sample. This number depends on the degree to which attributes of the class differ from those of other classes. In the case of white dwarfs, the RASS-XOR classifier trained with less than a hundred of these objects proved nevertheless to be quite effective both in detecting the majority of actual white dwarfs in the (training) sample of many thousand objects and ensuring high reliability of white dwarf candidates.

We anticipate that modifications to the classifier algorithm that note when objects do not map well into existing classes will be needed to improve its detection capabilities for previously unknown object types (Laidler & White 2003). Currently the latter functionality can be emulated through appropriate analyses of classification probabilities provided by ClassX.

Simple cross-identification procedures work well for the entire RASS and WGA samples. However, for X-ray sources more than a factor of 10 fainter (e.g., Chandra and XMM sources), we anticipate substantial incompleteness in the large optical surveys. The Sloan Survey should do better here.

Optical information is critical to distinguishing Galactic from extragalactic sources. It is less crucial for classifying clusters of galaxies and white dwarfs. The effect of infrared information in ClassX is generally similar to that from the optical in distinguishing broad classes. This information becomes increasingly useful in finer grained classification. A network of ClassX classifiers, each using a different set of object parameters (attributes) and even a different set of classes can provide a highly complete and reliable overall classification.

In general, the more detailed and accurate information is available to a classifier the more precise the classification results are.

The phase space of possible classifiers is very large. A substantial fraction of this effort was to learn a reasonable minimum of information to use.

Handling diverse sources of information is a major challenge. Adoption of standard protocols and formats such as those now being developed in the Virtual Observatory is crucial in creating a fast and easy-to-use system.

We wish to thank L. Angelini, M. E. Donahue, S. A. Drake, P. Fernique, F. Genova, W. D. Pence, M. Postman, M., and M. Wenger for numerous discussions of the project.

This work was funded through NASA's Applied Information Systems Research Program under grant NAG5-11019.

## REFERENCES

- Adelman, J. et al. 1999, BAAS 195, 8204
- Anderson, S. F. et al. 2003, AJ, 126, 2209
- Heath, D., Kasif, S., & Salzberg, S. 1996, in *Cognitive Technology: In Search of a Humane Interface*, eds. B. Gorayska & J. Mey (Amsterdam: Elsevier), p. 305
- Helfand, D. J., Schnee, S., Becker, R. H., White, R. L., & McMahon, R. G. 1999, ApJ, 117, 1568
- Laidler, V. G., & White, R. L. 2003, in *Statistical Challenges in Astronomy III*, eds. E. D. Feigelson & G. J. Babu (New York: Springer), p. 453
- Landt, H., Padovani, P., Perlman, E., Giommi, P., Bignall, H., & Tsiomis, A. 2001, MNRAS, 323, 757
- Monet, D. G., et al. 2003 AJ, 125, 984
- Murthy, S. K., Kasif, S., & Salzberg, S. 1994, J. Artif. Intell. Res., 2, 1
- Ochsenbein, F., Albrecht, M., Brighton, A., Fernique, P., Guillaume, D., Hanisch, R., & Wicenc, A. 2000, in *Astronomical Data Analysis Software and Systems IX*, Astron. Soc. Pacific Conference Series, N. Manset, C. Veillet, and D. Crabtree, eds., 216, 83. Also see <http://www.ivoa.net/twiki/bin/view/IVOA/IvoaVOTable> for updates to the VOTable standard.
- Ochsenbein, F., Bauer, P., & Marcout, J. 2000, A&AS 143, 230



- Odehahn, S. C. 1995, *PASP*, 107, 770
- Perlman, E. S., Padovani, P., Giommi, P., Sambruna, R., Jones, L., Tsiomis, A., & Reynolds, J. 1998, *AJ*, 115, 1253
- Rutledge, R., Brunner, R. J., & Prince, T.A. 2000, *ApJS* 131, 335
- Salzberg, S., Chandar, R., Ford, H., Murthy, S. K., & White, R. L. 1995, *PASP*, 107, 279
- Suchkov, A. A., Makarov, V. V., & Voges, W. 2003, *ApJ*, 595, 1206
- Voges, W. et al. 1999, *A&A*, 349, 389
- Voges, W. et al. 2000, *IAU Circ.*, 7432, 1
- Weir, N. et al. 1995, *PASP* 107, 1243
- White, R. L. et al. 2000, *ApJS*, 126, 133
- White, R. L. 1997, in *Statistical Challenges in Modern Astronomy II*, eds. G. J. Babu & E. D. Feigelson (New York: Springer), p. 135
- White, N. E., Giommi, P., Angelini, L. 2000, <http://wgacat.gsfc.nasa.gov>.
- White, R. L. 2000, in *ASP Conf. Ser.*, Vol. 216, *Astronomical Data Analysis Software and Systems IX*, eds. N. Manset, C. Veillet, & D. Crabtree (San Francisco: ASP), 577
- Zhang, Y. & Zhao, Y. 2003, *PASP* 115, 1005

Table 1. ‘Basic’ Classes and the Number of Class Objects in the WGACAT and RASS BSC Samples

Class	WGACAT		RASS	Origin of X-ray emission
	all	unique <sup>a</sup>		
Star .....	6027	4678	4694	Corona or shocked stellar wind.
WD (white dwarfs) ..	152	98	78	Hot atmosphere.
XRB (X-ray binaries) <sup>b</sup>	494	271	192	Accretion disk of a neutron star or black hole.
AGN <sup>c</sup> .....	4589	3031	726	Central accretion disk, XRBs, galactic wind
Galaxy .....	1614	1305	1015	XRBs, hot corona, galactic wind.
Cluster (of galaxies) .	1717	1508	210	Hot intracluster gas.
Unclassified .....	73986	65872	–	
Total .....	88579	76763	6915	

<sup>a</sup>In the case of multiple entries for a source, only the entry closest to the center of the PSPC field is included.

<sup>b</sup>Including cataclysmic variables.

<sup>c</sup>Including quasars, radio galaxies, and BL Lac galaxies.

Table 2. Class Attributes (Object Parameters) used by the Four ‘Basic’ ClassX Classifiers

Attribute name	Attribute Source	Classifier <sup>a</sup>	
		XOR	X
Galactic longitude, $l_{II}$ ..	Input	y	y
Galactic latitude, $b_{II}$ .....	Input	y	y
X-ray brightness <sup>b</sup> .....	X-ray data	y	y
Hardness ratio 1, $HR1$ <sup>c</sup> ..	X-ray data	y	y
Hardness ratio 2, $HR2$ <sup>c</sup> ..	X-ray data	y	y
X-ray extent (source size) <sup>d</sup>	X-ray data	y	y
Blue magnitude, $B$ <sup>e</sup> .....	Optical data	y	n
Red magnitude, $R$ <sup>e</sup> .....	Optical data	y	n
Radio counterpart flag <sup>f</sup> ..	Radio data	y	n

<sup>a</sup>X for WGACAT-X and RASS-X classifiers, XOR for WGACAT-XOR and RASS-XOR classifiers. Parameter required by a classifier is indicated by ‘y’, otherwise ‘n’.

<sup>b</sup>Defined as  $-2.5 \log(\text{count rate})$ .

<sup>c</sup>From RASS or computed from WGACAT.

<sup>d</sup>From RASS or ROSPSPC (for WGACAT) if available, else 0.

<sup>e</sup>From the USNO B1 catalog.

<sup>f</sup>1 if counterpart found in NVSS or SUMSS, else 0.

Table 3. Number of X-ray sources and number and average brightness of candidate counterparts selected in the nominal and control samples.

Sample	Number			$B_1^a$	$R_1^b$	$B_2^c$	$R_2^d$
	sources	candidates	sources with candidates	$N$	$N$	$N$	$N$
BSC nominal .	18,811	155,744	18,672	14.8 11,726	14.4 15,378	15.5 16,074	14.7 16,459
BSC offset ...	18,811	95,980	16,627	19.3 6,930	18.2 12,128	19.5 13,455	18.6 14401
FSC nominal .	105,924	736,879	101,559	18.2 51,573	17.3 77,229	18.6 84,463	17.7 89,014
FSC offset . . . .	105,924	592,531	95,507	19.2 43,027	18.1 70,427	19.5 77,799	18.5 83,369
WGA nominal	88,579	591,719	82,799	18.2 43,112	17.3 60,622	18.6 67,581	17.7 70,186
WGA offset ..	88,579	488,685	76,133	19.4 33,677	18.2 54,608	19.5 59,394	18.6 64,089

<sup>a</sup>The average first epoch  $B$  magnitude/the number of counterparts for which a first epoch  $B$  magnitude was defined (see Monet et al. 2003).

<sup>b</sup>Same as above but for the first epoch  $R$  magnitude.

<sup>c</sup>Same as above but for the second epoch  $B$  magnitude.

<sup>d</sup>Same as above but for the second epoch  $R$  magnitude.

Table 4. Cross-validation for the classifiers from RASS BSC and WGACAT

Input class		ClassX class					
Name	Number	STAR	WD	XRB	GALAXY	AGN	CLUSTER
RASS-X classifier							
STAR	4694....	4505	17	1	138	31	2
WD	78.....	8	65	0	2	2	1
XRB	192.....	119	10	52	6	3	2
GALAXY	1015....	651	6	4	261	59	34
AGN	726.....	528	2	0	111	84	1
CLUSTER	210.....	56	0	2	40	0	112
.....							
Total	6915....	5867	100	59	558	179	152
RASS-XOR classifier							
STAR	4675....	4629	0	1	45	0	0
WD	75.....	3	63	2	4	3	0
XRB	173.....	5	9	61	62	29	7
GALAXY	945.....	94	3	4	654	170	20
AGN	707.....	5	1	6	128	561	6
CLUSTER	188.....	3	0	4	52	25	104
.....							
Total	6763....	4739	76	78	945	788	137
WGACAT-X classifier							
STAR	4626....	3739	4	10	747	35	91
WD	67.....	38	11	1	14	0	3
XRB	265.....	121	1	61	72	2	8
GALAXY	1281....	370	0	1	557	166	187
AGN	3012....	579	0	8	2189	60	176
CLUSTER	1496....	356	0	3	699	101	337
.....							
Total	10747...	5203	16	84	4278	364	802
WGACAT-XOR classifier							
STAR	4028....	3617	1	7	279	51	73
WD	59.....	25	4	3	25	0	2
XRB	239.....	87	0	76	66	2	8
GALAXY	962.....	267	0	2	307	276	110
AGN	2648....	144	0	6	2195	95	208
CLUSTER	1311....	170	0	6	599	67	469
.....							
Total	9247....	4310	5	100	3471	491	870

Table 5. Classification of RASSBSC by the RASS-X classifier<sup>a</sup>

RASSBSC Source Name	Class Index	P(Star)	P(WD)	P(XRB)	P(Galaxy)	P(AGN)	P(Cluster)	Class Name
1RXS J000007.0+081653	3	0.290	0.007	0.038	0.445	0.176	0.044	Galaxy
1RXS J000011.9+052318	0	0.666	0.003	0.023	0.142	0.126	0.040	Star
1RXS J000012.6+014621	0	0.702	0.002	0.022	0.125	0.117	0.031	Star
1RXS J000013.5+575628	0	0.871	0.001	0.017	0.060	0.047	0.003	Star
1RXS J000038.4+794037	0	0.888	0.001	0.015	0.049	0.044	0.003	Star
1RXS J000042.5+621034	0	0.888	0.001	0.015	0.049	0.044	0.003	Star
1RXS J000055.5+172346	0	0.819	0.001	0.018	0.076	0.072	0.014	Star
1RXS J000115.6+705535	0	0.871	0.001	0.017	0.060	0.047	0.003	Star
1RXS J000119.8+501659	0	0.696	0.005	0.067	0.111	0.098	0.023	Star
1RXS J000123.3+272241	0	0.888	0.001	0.015	0.049	0.044	0.003	Star

<sup>a</sup>Table 5 is given in its entirety at the ClassX web site, <http://heasarc.gsfc.nasa.gov>. A portion shown here is for guidance regarding its format and content.

Table 6. Classification of WGACAT by the WGACAT-XOR classifier<sup>a</sup>

WGACAT Source Name	P(Star)	P(WD)	P(XRB)	P(Galaxy)	P(AGN)	P(Cluster)	Class Name	ROSPSPC counterpart?
1WGA J1055.2+5638	0.483	0.039	0.061	0.057	0.254	0.106	Star	n
1WGA J1049.6+5641	0.483	0.039	0.061	0.057	0.254	0.106	Star	n
1WGA J1053.8+5709	0.270	0.039	0.039	0.219	0.348	0.085	AGN	y
1WGA J1053.2+5718	0.265	0.035	0.035	0.209	0.405	0.050	AGN	y
1WGA J1052.9+5725	0.415	0.022	0.026	0.160	0.332	0.045	Star	y
1WGA J1051.3+5725	0.483	0.039	0.061	0.057	0.254	0.106	Star	y
1WGA J1751.8-3450	0.233	0.026	0.028	0.375	0.291	0.047	Galaxy	y
1WGA J1415.2+1119	0.233	0.026	0.028	0.375	0.291	0.047	Galaxy	y
1WGA J1415.2+1119	0.352	0.037	0.141	0.046	0.311	0.115	Star	n
1WGA J1415.0+1119	0.238	0.031	0.032	0.290	0.347	0.062	AGN	y

<sup>a</sup>Table 6 is given in its entirety at the ClassX web site, <http://heasarc.gsfc.nasa.gov>. A portion shown here is for guidance regarding its format and content.